

# Reversible Interconversion between Singlet and Triplet 2-Naphthyl(carbomethoxy)carbene

Zhendong Zhu,<sup>†,‡</sup> Thomas Bally,<sup>\*,†</sup> Louise L. Stracener,<sup>§</sup> and Robert J. McMahon<sup>\*,§</sup>

Contribution from the Institute of Physical Chemistry, University of Fribourg, P erolles, CH-1700 Fribourg, Switzerland, and Department of Chemistry, University of Wisconsin, Madison, Wisconsin 53706-1396

Received September 14, 1998

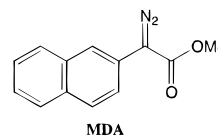
**Abstract:** Photolysis of methyl  $\alpha$ -diazo-(2-naphthyl)acetate at 450 nm yields primarily the triplet ground state of 2-naphthyl(carbomethoxy)carbene ( $^3\text{NCC}$ ), which was characterized by its UV/visible, IR, and ESR spectra as well as by trapping with  $\text{O}_2$  and  $\text{CO}$ . Bleaching of the weak visible bands of  $^3\text{NCC}$  ( $\lambda > 515$  nm) leads to the disappearance of the triplet ESR spectrum and to a new optical spectrum with broad bands in the near-UV region. The spectra of  $^3\text{NCC}$  can be almost fully recovered in the dark at 12 K. The same process also occurs upon irradiation at 450 nm, with the exception that the recovery of  $^3\text{NCC}$  is accompanied by the formation of small amounts of 2-naphthyl(methoxy)ketene and 2-(2-naphthyl)propiolactone. The observed optical and IR spectra of the intermediate that is formed reversibly from  $^3\text{NCC}$  are in full accord with quantum chemical model calculations for the singlet state of the same carbene  $^1\text{NCC}$ , but *not* with the tricyclic cyclopropene derivative observed previously for the parent 2-naphthylcarbene or the 1-(2-naphthyl)-2-methoxyoxirene. Exploration of the potential energy surfaces for singlet and triplet NCC show that a barrier between the two states is created by a pronounced change in conformation of the carbomethoxy group, which may furthermore be hindered in a solid matrix environment.

## Introduction

Thermal and photochemical rearrangements of  $\alpha$ -diazocarbonyl compounds to ketenes (Wolff rearrangement) have received considerable attention because of their relevance to both fundamental science<sup>1–10</sup> and applied technology.<sup>11–13</sup> In synthetic organic chemistry, the Wolff rearrangement represents the key step in the Arndt–Eistert sequence for the one-carbon homologation of carboxylic acids.<sup>1–7</sup> The rearrangement also serves as an excellent method for effecting ring contraction and is notable for its success in forming strained rings.<sup>1–6,8</sup> Recent applications of the Wolff rearrangement involve the use of  $\alpha$ -diazo ketones as photochemically triggered DNA-cleaving

reagents.<sup>9,10</sup> The most important application of the Wolff rearrangement derives from the use of  $\alpha$ -diazocarbonyl compounds in computer circuit microfabrication.<sup>11–14</sup>

Mechanistically, the Wolff rearrangement raises intriguing questions concerning the intimate details of the transformation from  $\alpha$ -diazocarbonyl compound to products and the nature of the various intermediates that may or may not be involved (vide infra).<sup>2–6</sup> Key mechanistic issues concerning this chemical transformation remain unresolved or controversial. Rather than trying to extrapolate between results obtained from a variety of  $\alpha$ -diazocarbonyl compounds, each optimized for a particular type of chemical or spectroscopic investigation, we sought a system in which a diverse array of experimental methods could be brought to bear on the study of a *single*  $\alpha$ -diazocarbonyl species. The current article, in conjunction with two companion articles,<sup>15,16</sup> describes a comprehensive experimental and computational investigation of the rearrangements derived upon photolysis of the  $\alpha$ -diazocarbonyl compound, methyl  $\alpha$ -diazo-(2-naphthyl)acetate (MDA).



**Background.** During the past 35 years, the mechanism of the Wolff rearrangement has been the subject of extensive

<sup>†</sup> University of Fribourg.

<sup>‡</sup> Present address: Department of Chemistry, The Ohio State University, Columbus, OH 43210.

<sup>§</sup> University of Wisconsin.

(1) Ye, T.; McKervey, A. M. *Chem. Rev.* **1994**, *94*, 1091.

(2) Maas, G. In *Methoden der Organischen Chemie (Houben-Weyl)*; Regitz, M., Ed.; Thieme Verlag: Stuttgart, 1989; Vol. 19b/2; p 1022.

(3) Regitz, M.; Maas, G. *Diazo Compounds*; Academic Press: Orlando, FL, 1986.

(4) Meier, H.; Zeller, K.-P. *Angew. Chem., Int. Ed. Engl.* **1975**, *14*, 32.

(5) Jones, M.; Moss, R. A. *Carbenes*; Wiley: New York, 1973; Vols. I and II.

(6) Kirmse, W. *Carbene Chemistry*, 2nd ed.; Academic Press: New York, 1971.

(7) March, J. *Advanced Organic Chemistry*; Wiley: New York, 1992; p 1083.

(8) Redmore, D.; Gutsche, C. D. *Adv. Alicyclic. Chem.* **1971**, *3*, 125.

(9) Nakatani, K.; Maekawa, S.; Tanabe, K.; Saito, I. *J. Am. Chem. Soc.* **1995**, *117*, 10635.

(10) Nakatani, K.; Shirai, J.; Sando, S.; Saito, I. *J. Am. Chem. Soc.* **1997**, *119*, 7626.

(11) Reichmanis, E.; Thompson, L. F. *Chem. Rev.* **1989**, *89*, 1273.

(12) Reiser, A. *Photoreactive Polymers: The Science and Technology of Resists*; Wiley: New York, 1989.

(13) Steppan, H.; Buhr, G.; Vollman, H. *Angew. Chem., Int. Ed. Engl.* **1982**, *21*, 455.

(14) Moreau, W. M. *Semiconductor Lithography*; Plenum Press: New York, 1988.

(15) Wang, Y.; Yuzawa, T.; Hamaguchi, H.; Toscano, J. P. *J. Am. Chem. Soc.* **1999**, *121*, xxxx.

(16) Wang, J.-L.; Lithovarik, I.; Platz, M. S. *J. Am. Chem. Soc.* **1998**, *121*, xxxx.

investigation.<sup>2–6</sup> The relationship between the conformation of the  $\alpha$ -diazocarbonyl compound (*s-E* or *s-Z*) and the rate of Wolff rearrangement led to the suggestion that the rearrangement proceeds in a concerted manner from the *s-E* conformer but in a stepwise manner from the *s-Z* conformer.<sup>17–21</sup> In instances where the Wolff rearrangement proceeds in a stepwise manner,<sup>20,21</sup> decomposition of the  $\alpha$ -diazocarbonyl compound affords entry into an interesting potential energy surface containing  $\alpha$ -carbonyl carbene, oxirene, and ketene intermediates. Each of these intermediates has been the subject of confusion and controversy to experimentalists and theorists alike.

$\alpha$ -Carbonylcarbenes generally possess triplet electronic ground states, consistent with ESR detection<sup>22–31</sup> and computational predictions.<sup>32–36</sup> In several instances, triplet  $\alpha$ -carbonylcarbenes have also been observed by IR<sup>26,28,29,37,38</sup> and UV/visible spectroscopy.<sup>26,31,37,39</sup> In contrast to the relatively well characterized triplet ground state, the lowest singlet state remains the subject of uncertainty. Calculations predict that the lowest singlet state of carboxyhydroxy carbene, H–C–COOH (H–C–O dihedral angle  $\sim 90^\circ$ ), lies  $\sim 4.7$  kcal/mol above the planar triplet ground state.<sup>36</sup>

The closed-shell singlet states of  $\alpha$ -carbonylcarbenes connect adiabatically to the corresponding oxirenes. These  $4\pi$ -electron antiaromatic species have proven to be exceptionally elusive,<sup>40,41</sup> although their involvement in the Wolff rearrangement has been inferred from isotope label scrambling experiments,<sup>42–48</sup> keto-

carbene–ketocarbene equilibration studies,<sup>49–52</sup> and neutralization of gas-phase radical ions.<sup>53–55</sup> Claims for the direct observation of various oxirene intermediates<sup>56–58</sup> remain critically unsubstantiated.<sup>59,60</sup> At the current time, the most persuasive case for the experimental observation of an oxirene rests with dimethyloxirene.<sup>61–63</sup>

A reason why oxirenes have so far escaped unambiguous detection is that the potential energy surfaces connecting them to  $\alpha$ -carbonylcarbenes are very flat. Recent very reliable ab initio calculations led to the conclusion that, for the parent formyl carbene, H–C–CHO, which is almost isoenergetic to the parent oxirene, the surface is so flat that minimums and transition states can no longer be clearly distinguished because inclusion of zero-point energies changes their energy ordering.<sup>64</sup> Electron-releasing substituents on the carbene center are expected to stabilize the electron-deficient  $\alpha$ -carbonyl carbene and destabilize the electron-rich oxirene,<sup>64</sup> thus enhancing the likelihood that the oxirene becomes a transition state for the interconversion of the two  $\alpha$ -carbonylcarbenes.

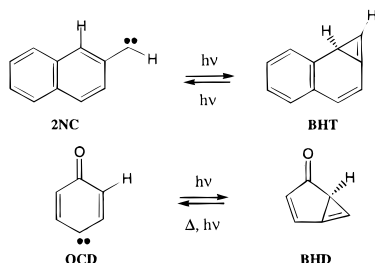
Despite the elusive character of singlet  $\alpha$ -carbonylcarbenes, lifetimes and rate constants for their conversion to ketenes (Wolff rearrangement) have been determined using the pyridinium ylide method to reveal the solution kinetics of the spectroscopically invisible singlet carbenes.<sup>65–67</sup> Of the various reactive intermediates on this potential energy surface, ketenes represent the most well characterized species.<sup>68</sup> Even so, a detailed understanding of the kinetics of hydration, involving carboxylic acid enols, emerged only recently.<sup>60,69</sup> A retro-Wolff rearrangement of a ketene to an  $\alpha$ -carbonyl carbene may occur

- (17) Kaplan, F.; Meloy, G. K. *J. Am. Chem. Soc.* **1966**, *88*, 950.  
 (18) Kaplan, F.; Mitchell, M. L. *Tetrahedron Lett.* **1979**, 759.  
 (19) Roth, H. D. *Acc. Chem. Res.* **1977**, *10*, 85.  
 (20) Tomioka, H.; Hayashi, N.; Asano, T.; Izawa, Y. *Bull. Chem. Soc. Jpn.* **1983**, *56*, 758 and references therein.  
 (21) Torres, M.; Ribo, J.; Clement, A.; Strausz, O. P. *Can. J. Chem.* **1983**, *61*, 996.  
 (22) Moriconi, E. J.; Murray, J. J. *J. Org. Chem.* **1964**, *29*, 3577.  
 (23) Trozzolo, A. M. *Acc. Chem. Res.* **1968**, *1*, 329.  
 (24) Hutton, R. S.; Roth, H. D. *J. Am. Chem. Soc.* **1978**, *100*, 4324.  
 (25) Roth, H. D.; Hutton, R. S. *Tetrahedron* **1985**, *41*, 1567.  
 (26) McMahon, R. J.; Chapman, O. L.; Hayes, R. A.; Hess, T. C.; Krimmer, H. P. *J. Am. Chem. Soc.* **1985**, *107*, 7597.  
 (27) Murai, H.; Safarik, I.; Torres, M.; Strausz, O. P. *J. Am. Chem. Soc.* **1988**, *110*, 1025.  
 (28) Tomioka, H.; Hirai, K.; Tabayashi, K.; Murata, S.; Izawa, Y.; Inagaki, S.; Okajima, T. *J. Am. Chem. Soc.* **1990**, *112*, 7692.  
 (29) Murata, S.; Yamamoto, T.; Tomioka, H. *J. Am. Chem. Soc.* **1993**, *115*, 4013.  
 (30) Sander, W.; Bucher, G.; Wierlacher, S. *Chem. Rev.* **1993**, *93*, 1583.  
 (31) Fujiwara, Y.; Tanimoto, Y.; Itoh, M.; Hirai, K.; Tomioka, H. *J. Am. Chem. Soc.* **1987**, *109*, 942.  
 (32) Tanaka, K.; Yoshimine, M. *J. Am. Chem. Soc.* **1980**, *102*, 7655.  
 (33) Baird, N. C.; Taylor, K. F. *J. Am. Chem. Soc.* **1978**, *100*, 1333.  
 (34) Gosavi, R.; Torres, M.; Strausz, O. P. *Can. J. Chem.* **1991**, *69*, 1630.  
 (35) Kim, K. S.; Schaefer, H. F. *J. Am. Chem. Soc.* **1980**, *102*, 5390.  
 (36) Xie, Y.; Schaefer, H. F. *Mol. Phys.* **1996**, *87*, 389.  
 (37) Zhu, Z. Thesis No. 1152, University of Fribourg, 1997.  
 (38) Using picosecond infrared spectroscopy (20-ps time resolution), Lippert et al. were unable to observe an IR transient preceding ketene formation upon irradiation of diazo Meldrum's acid in a poly(methyl methacrylate) film: Lippert, T.; Koskelo, A.; Stoutland, P. O. *J. Am. Chem. Soc.* **1996**, *118*, 1551.  
 (39) In several flash photolysis studies, transient UV absorptions have been assigned to arylcarbomethoxycarbene intermediates (spin multiplicity not specified): (a) Chiang, Y.; Kresge, A. J.; Pruszyński, P.; Shepp, N. P.; Wirz, J. *Angew. Chem., Int. Ed. Engl.* **1991**, *30*, 1366. (b) Shepp, N. P.; Wirz, J. *J. Am. Chem. Soc.* **1994**, *116*, 11749. (c) Vleggaar, J. J. M.; Huizer, A. H.; Kraakman, A.; Nijssen, W. P. M.; Visser, R. J.; Varma, C. A. G. O. *J. Am. Chem. Soc.* **1994**, *116*, 11754.  
 (40) Lewars, E. G. *Chem. Rev.* **1983**, *83*, 519.  
 (41) Torres, M.; Lown, E. M.; Gunning, H. E.; Strausz, P. P. *Pure Appl. Chem.* **1980**, *52*, 1623.  
 (42) Csizmadia, I. G.; Font, J.; Strausz, O. P. *J. Am. Chem. Soc.* **1968**, *90*, 7360.  
 (43) Russell, R. L.; Rowland, F. S. *J. Am. Chem. Soc.* **1970**, *92*, 7508.  
 (44) Montague, D. C.; Rowland, F. S. *J. Am. Chem. Soc.* **1971**, *93*, 5381.  
 (45) Zeller, K.-P. *Angew. Chem., Int. Ed. Engl.* **1977**, *16*, 781.  
 (46) Zeller, K.-P. *Chem. Ber.* **1979**, *112*, 678.

- (47) Moore, C. B. *Discuss. Faraday Soc.* **1995**, *102*, 1 and references therein.  
 (48) Oxirene participation depends on the substrate and reaction conditions. In several instances, isotope labeling experiments exclude the involvement of oxirenes. For examples, see: (a) Majerski, Z.; Redvanly, C. S. *J. Chem. Soc., Chem. Commun.* **1972**, 69. (b) Matlin, S. A.; Sammes, P. G. *J. Chem. Soc., Perkin Trans. 1* **1973**, 2851. (c) Timm, U.; Zeller, K.-P.; Meier, H. *Tetrahedron* **1977**, *33*, 453.  
 (49) Matlin, S. A.; Sammes, P. G. *J. Chem. Soc., Perkin Trans. 1* **1972**, 2623.  
 (50) Timm, U.; Zeller, K.-P.; Meier, H. *Chem. Ber.* **1978**, *111*, 1549.  
 (51) Cormier, R. A. *Tetrahedron Lett.* **1980**, *21*, 2021.  
 (52) Tomioka, H.; Okuno, H.; Kondo, S.; Izawa, Y. *J. Am. Chem. Soc.* **1980**, *102*, 7123.  
 (53) Baar, B. L. M. v.; Heinrich, N.; Koch, W.; Postma, R.; Terlouw, J. K.; Schwarz, H. *Angew. Chem., Int. Ed. Engl.* **1987**, *26*, 140.  
 (54) Hop, C. E. C. A.; Holmes, J. L.; Terlouw, J. K. *J. Am. Chem. Soc.* **1989**, *111*, 441.  
 (55) Turecek, F.; Drinkwater, D. E.; McLafferty, F. W. *J. Am. Chem. Soc.* **1991**, *113*, 5958.  
 (56) Torres, M.; Bourdelande, J. L.; Clement, A.; Strausz, O. P. *J. Am. Chem. Soc.* **1983**, *105*, 1698.  
 (57) Tanigaki, K.; Ebbesen, T. W. *J. Am. Chem. Soc.* **1987**, *109*, 5883.  
 (58) Tanigaki, K.; Ebbesen, T. W. *J. Phys. Chem.* **1989**, *93*, 4531.  
 (59) Laganis, E. D.; Janik, D. S.; Curphey, T. J.; Lemal, D. M. *J. Am. Chem. Soc.* **1983**, *105*, 7457.  
 (60) Chiang, Y.; Kresge, A. J.; Popik, V. V.; Shepp, N. P. *J. Am. Chem. Soc.* **1997**, *119*, 10203 and references therein.  
 (61) Debù, F.; Monnier, M.; Verlaque, P.; Davidovics, G.; Pourcin, J.; Bodot, H.; Aycard, J.-P. *C. R. Acad. Sci., Ser. 2* **1986**, *303*, 897.  
 (62) Bachmann, C.; N-Guessan, T. Y.; Debù, F.; Monnier, M.; Pourcin, J.; Aycard, J.-P.; Bodot, H. *J. Am. Chem. Soc.* **1990**, *112*, 7488.  
 (63) Fowler, J. E.; Galbraith, J. M.; Vacek, G.; Schaefer, H. F. *J. Am. Chem. Soc.* **1994**, *116*, 9311.  
 (64) Scott, A. P.; Nobes, R. H.; Schaefer, H. F.; Radom, L. *J. Am. Chem. Soc.* **1994**, *116*, 10159.  
 (65) Toscano, J. P.; Platz, M. S.; Nikolaev, V. *J. Am. Chem. Soc.* **1994**, *116*, 8146.  
 (66) Toscano, J. P.; Platz, M. S.; Nikolaev, V. *J. Am. Chem. Soc.* **1995**, *117*, 4712.  
 (67) Wang, J.-L.; Toscano, J. P.; Platz, M. S.; Nikolaev, V.; Popik, V. *J. Am. Chem. Soc.* **1995**, *117*, 5477.  
 (68) Tidwell, T. T. *Ketenes*; Wiley-Interscience: New York, 1995.  
 (69) Andraos, J.; Chiang, Y.; Kresge, A. J.; Popik, V. V. *J. Am. Chem. Soc.* **1997**, *119*, 8417.

under conditions of photolysis or thermolysis.<sup>70</sup> In the gas phase, sophisticated spectroscopic investigations of the parent ketene by Moore and co-workers provide unprecedented insight into the detailed photochemistry and molecular dynamics on the C<sub>2</sub>H<sub>2</sub>O potential energy surface.<sup>47</sup>

Finally, the issue of vinylcarbene–cyclopropene interconversion pertains to the discussion of our particular substrate, 2-naphthyl(carbomethoxy)carbene (NCC). Triplet 2-naphthylcarbene (2NC) can be reversibly interconverted by a vinylcar-



bene–cyclopropene rearrangement with 2,3-benzobicyclo[4.1.0]-hepta-2,4,6-triene (BHT).<sup>71</sup> A similar type of interconversion had been found earlier for triplet 4-oxo-2,5-cyclohexadienylidene (OCD) and 1*H*-bicyclo[3.1.0]hexa-3,5-dien-2-one (BHD),<sup>72,73</sup> except that the reconversion of BHD to the triplet carbene also occurred thermally in this case. This is in contrast to BHT, which is thermally stable. Actually, very little is known about the spectroscopic properties of singlet carbenes with triplet ground states, because the singlets usually cannot be observed due to fast intersystem crossing to the ground state. We believe that we have found an exception to this rule, and this paper summarizes the evidence we have obtained for this interesting system.

## Methods

**Synthesis.** Methyl  $\alpha$ -diazo-(2-naphthyl)acetate (MDA) was prepared by the diazo transfer method as modified by Davies et al.<sup>74</sup> and purified by repeated recrystallization to give dark orange crystals.

**Matrix Isolation.** For the UV/visible and IR experiments, a few ground crystals of MDA were placed in a U-tube just before the inlet system of the cryostat (Air Products CSW 200). After evacuation, the temperature of the U-tube was kept at 40 °C in a water bath while the parts of the inlet system leading to the cryostat were warmed to 50 °C with a heating tape to prevent condensation. During matrix isolation, the temperature of the water bath was adjusted to permit the argon (mixed occasionally with some nitrogen to enhance the optical quality of the matrixes) flowing through the U-tube to carry along appropriate quantities of MDA to form a matrix giving reasonable optical densities of precursor and products (which depend on the intensity of the bands to be monitored). Deazotation of MDA was effected by irradiation with the light of an argon plasma lamp (GAT PB 1500) passing through a 450  $\pm$  30 nm interference filter. The lamp was also used with appropriate filters for the subsequent photolyses, along with a medium-pressure Hg/Xe lamp with a 313-nm interference filter for irradiations at that wavelength.

For the ESR experiments, samples of matrix-isolated MDA were prepared by vapor-phase co-deposition of MDA (sublimed at 75 °C,

(70) Qiao, G. G.; Meutermaans, W.; Wong, M. W.; Träubel, M.; Wentrup, C. *J. Am. Chem. Soc.* **1996**, *118*, 3852.

(71) Albrecht, S. W.; McMahon, R. J. *J. Am. Chem. Soc.* **1993**, *115*, 855.

(72) (a) Sander, W.; Müller, W.; Sustmann, R. *Angew. Chem., Int. Ed. Engl.* **1988**, *27*, 572. (b) Sander, W.; Bucher, G.; Reichel, F.; Cremer, D. *J. Am. Chem. Soc.* **1991**, *113*, 5311.

(73) Solé, A.; Olivella, S.; Bofill, J. M.; Anglada, J. M. *J. Phys. Chem.* **1995**, *99*, 5934.

(74) Davies, H. M.; Clark, T. J.; Smith, H. D. *J. Org. Chem.* **1991**, *56*, 3817.

10<sup>-7</sup> Torr) and argon.<sup>26,75</sup> Irradiations were performed using a 300-W high-pressure Xe arc lamp. Wavelength control was provided using either glass cutoff filters ( $\lambda > 534$  nm, Corning 3-67) or a Spectral Energy GM252 high-intensity monochromator (16-nm band-pass centered on the specified value).

**Spectroscopy.** Optical spectra were measured on a Perkin-Elmer Lambda 19 instrument (200–2000 nm), IR spectra with a Bomem DA3 FT interferometer (150–4000 cm<sup>-1</sup>), and ESR spectra on a Bruker ESP 300E instrument (X-band).<sup>26,75</sup> All UV/visible and IR spectra are given in absorbance.

**Calculations.** On the basis of recent gratifying experiences in our laboratories<sup>76</sup> as well as others that study carbenes computationally,<sup>77–79</sup> we decided to use the B3LYP hybrid density functional method<sup>80</sup> with the 6-31G\* basis set throughout, after verifying that the results of such calculations are in good accord with those obtained at highly correlated coupled cluster levels for the parent carbomethoxycarbene, H–C–COOCH<sub>3</sub>.<sup>37</sup> Unless otherwise explicitly noted, the geometries of all species for which theoretical results are reported in this study were optimized under no constraints. The nature of all stationary points was assessed by frequency calculations which were also used in the assignment of the IR spectra for the stable species. The above calculations were carried out with the Gaussian 92 and 94 suite of programs.<sup>81</sup> Electronic structure calculations were effected at the B3LYP/6-31G\* geometries by the INDO/S-CI procedure<sup>82</sup> with the ZINDO program.<sup>83</sup>

## Experimental Results

Upon photolysis in Ar at 450 nm, the optical spectrum of the diazo compound, MDA, (spectrum a in Figure 1) gave way to a new one with several new peaks above 350 nm (spectrum b and difference spectrum b – a in Figure 1). Simultaneously, the IR bands of MDA, notably the strong 2100-cm<sup>-1</sup> diazo peak, diminished significantly and were replaced by distinct new ones at ~2120, 1846, and 1660 cm<sup>-1</sup>, in addition to a group of intense peaks around 1200 cm<sup>-1</sup> (difference spectrum b – a in Figure 2). Under similar conditions, ESR spectroscopy revealed the appearance of signals ascribable to two conformational isomers of a triplet carbene (Figure 3a), one giving rise to higher-field transitions (**A**) and the other displaying similar transitions at lower field (**B**).

Subsequent irradiation at >515 nm led to the disappearance of the newly formed visible peaks (spectrum c – b in Figure 1), the IR absorption at 1660 cm<sup>-1</sup>, and the group near 1200 cm<sup>-1</sup> (spectrum c – b in Figure 2), and the triplet ESR signals (Figure 3b, note that the conformational isomer **B** disappears more rapidly than conformer **A**). During this irradiation, a broad, near-UV absorption at 400–450 nm plus a sharper band at ~340 nm appeared in the optical spectrum, and peaks at 1590 and

(75) Seburg, R. A.; McMahon, R. J. *J. Am. Chem. Soc.* **1992**, *114*, 7183.

(76) Matzinger, S.; Bally, T.; Patterson, E. V.; McMahon, R. J. *J. Am. Chem. Soc.* **1996**, *118*, 1535.

(77) Schreiner, P. R.; Karney, W. L.; Schleyer, P. v. R.; Borden, W. T.; Hamilton, T. P.; Schaefer, H. F. *J. Org. Chem.* **1996**, *61*, 7030.

(78) Xie, Y.; Schreiner, P. R.; Schleyer, P. v. R.; Schaefer, H. F. *J. Am. Chem. Soc.* **1997**, *119*, 1370.

(79) Wong, M. W.; Wentrup, C. *J. Org. Chem.* **1996**, *61*, 7022.

(80) For a description of this and other density functional methods implemented in the Gaussian series of programs, see: Johnson, B. G.; Gill, P. M. W.; Pople, J. A. *J. Chem. Phys.* **1993**, *98*, 5612.

(81) Frisch, M. J.; Trucks, G. W.; Schlegel, H. B.; Gill, P. M. W.; Johnson, B. G.; Robb, M. A.; Cheeseman, J. R.; Keith, T.; Petersson, G. A.; Montgomery, J. A.; Raghavachari, K.; Al-Laham, M. A.; Zakrzewski, V. G.; Ortiz, J. V.; Foresman, J. B.; Cioslowski, J.; Stefanov, B. B.; Nanayakkara, A.; Challacombe, M.; Peng, C. Y.; Ayala, P. Y.; Chen, W.; Wong, M. W.; Andres, J. L.; Repogle, E. S.; Gomperts, R.; Martin, R. L.; Fox, D. J.; Binkley, J. S.; DeFrees, D. J.; Baker, J.; Stewart, J. P.; Head-Gordon, M.; Gonzales, M. C.; Pople, J. A. Gaussian Program, Gaussian 94, Rev. B1 and D4, Gaussian, Inc.: Pittsburgh, PA, 1995.

(82) Zerner, M. C.; Ridley, J. E. *Theor. Chim. Acta* **1973**, *32*, 111.

(83) Zerner, M. C. ZINDO, Quantum Theory Project, University of Florida, Gainesville, 1985.

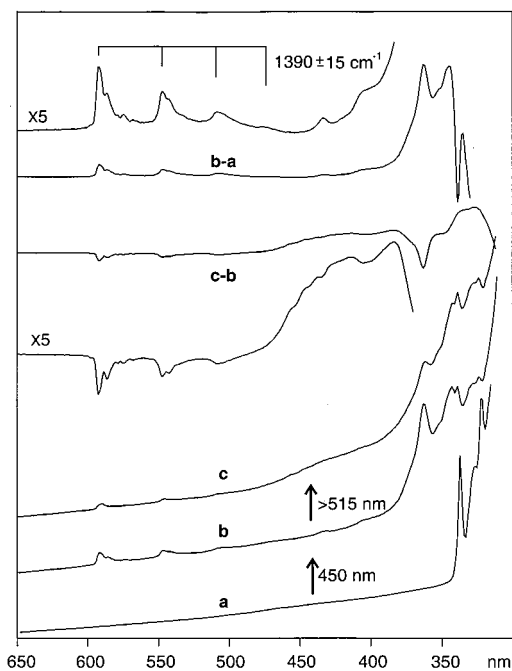


**Figure 1.** Changes in the optical spectra upon photodeazetation of the diazo compound MDA (a) by 450-nm irradiation (b and b – a) and subsequent >515-nm bleaching of the corresponding absorptions (c and c – b). “X5” refers to spectra expanded by a factor of 5.

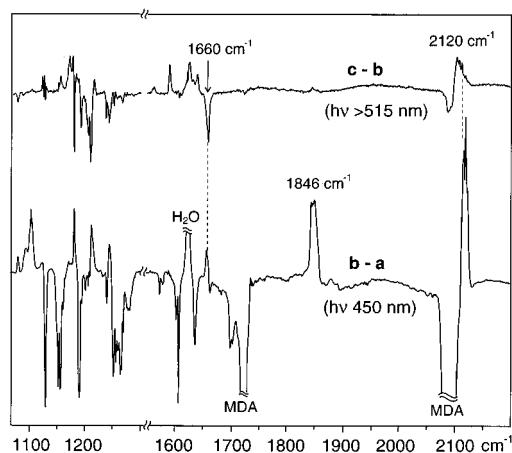


**Figure 2.** Changes in the IR spectra upon photodeazetation of the diazo compound MDA by 450-nm irradiation (b – a) and subsequent >515-nm bleaching of the corresponding absorptions (c – b).

$1625\text{ cm}^{-1}$  appeared, along with some changes around  $1200\text{ cm}^{-1}$ , in the IR spectrum (cf. spectra c – b in Figures 1 and 2). The  $2120\text{-cm}^{-1}$  band increased slightly, whereas the intensity of the  $1846\text{-cm}^{-1}$  band remained constant.

This photoconversion effected at  $>515\text{ nm}$  was found to be reversible under both photochemical and thermal conditions. Thus, renewed irradiation at  $450\text{ nm}$  led to the almost complete reappearance of all the spectroscopic features formed originally on photodeazotation of MDA. In fact, the difference spectra obtained on 450- and  $>515\text{-nm}$  irradiations show an almost perfect mirror-image relationship, both in the UV/visible and in the IR range (Figure 4), provided that the bleaching of MDA had been carried to completion in the first photolysis. In the ESR experiment, isomer **B** reappeared more rapidly than isomer **A** (Figure 3c).

Interestingly, we found the thermal reaction by coincidence when we kept a sample that was irradiated at  $>515\text{ nm}$  (Figure 1, spectrum c) in the dark overnight at 12 or 16 K. The

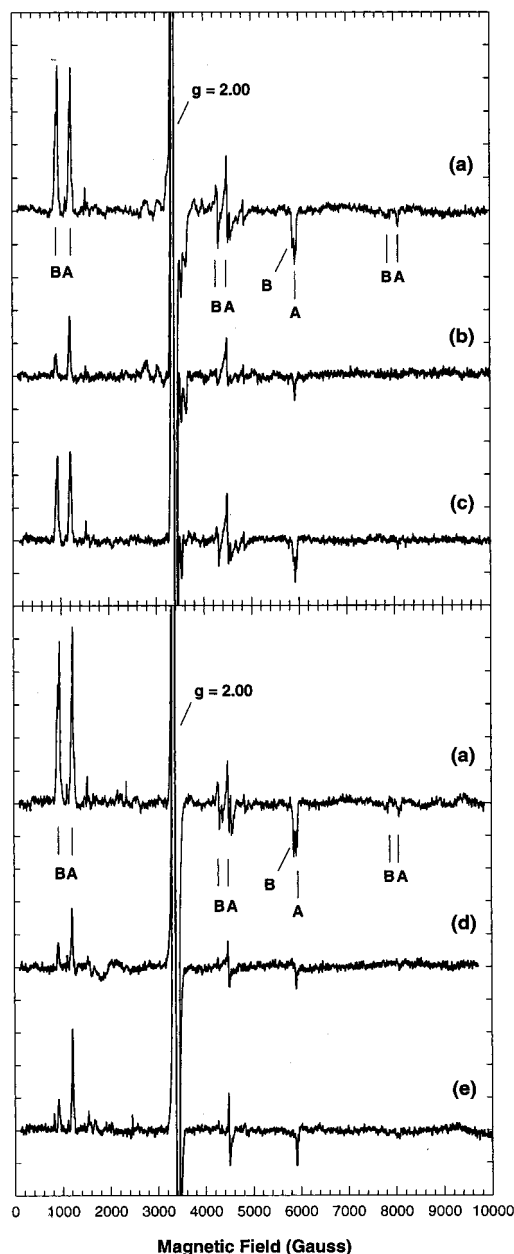


**Figure 3.** Triplet ESR spectra in argon at 16 K: (a)  $^3\text{NCC}$  obtained upon photolysis of MDA ( $\lambda = 313\text{ nm}$ ; 48 h); (b) bleaching of  $^3\text{NCC}$  ( $\lambda > 534\text{ nm}$ , 11.75 h); (c) reappearance of  $^3\text{NCC}$  upon irradiation ( $\lambda = 450\text{ nm}$ , 17.5 h); (d) bleaching of  $^3\text{NCC}$  ( $\lambda > 534\text{ nm}$ , 7 h); (e) reappearance of  $^3\text{NCC}$  upon standing in the dark (16 K, 48 h).

corresponding changes are documented in Figures 3 (ESR) and 5 (optical/IR), and it is readily seen that they are almost identical to those observed on photolysis at  $450\text{ nm}$  (cf. Figure 4). In contrast to the photochemical reaction, however, conformer **A** appeared more rapidly than conformer **B** (Figure 3e). Again, the thermal changes could be reversed by  $>515\text{-nm}$  irradiation (Figure 5, spectrum b).

When the above experiments were carried out in matrixes doped with 0.2%  $\text{O}_2$ , a new band with  $\lambda_{\text{max}} = 420\text{ nm}$  formed upon photocleavage of MDA. The intensity of this absorption increased considerably on annealing of the matrix to 35 K while the group of sharp bands at  $500\text{--}600\text{ nm}$  and the sharp peak at  $360\text{ nm}$  decreased (spectrum a in Figure 6). Although this band was also readily bleached by  $450\text{-nm}$  irradiation (spectrum b), the spectroscopic features associated with the first photoproduct did *not* reappear concomitantly, as they did in the absence of

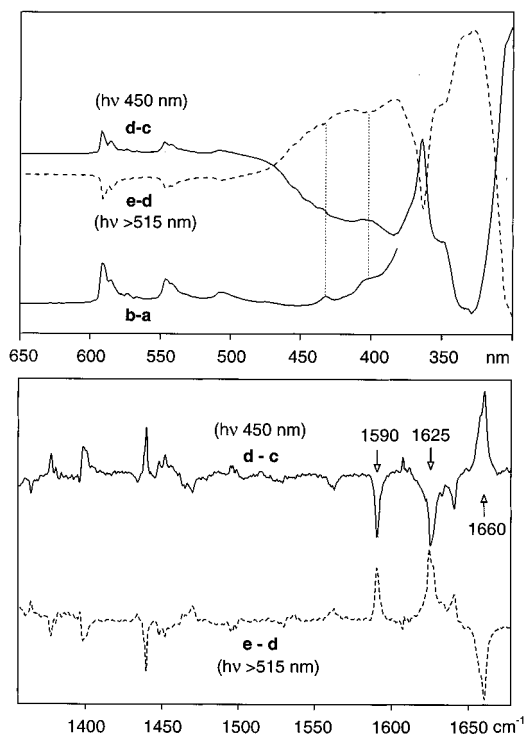


**Figure 4.** Changes in the optical spectra (top) and the IR spectra (bottom) on 450-nm photolysis of the sample giving spectrum c in Figure 1 (d – c) and subsequent >515-nm photolysis (e – d). The expanded optical spectrum b – a is reproduced from Figure 1 for reference purpose. Note that the bumps at 405 and 435 nm in spectrum e – d are due to absorptions of the species being bleached.

oxygen. When the sample was subjected to >515-nm photolysis prior to annealing, the growth of the 420-nm band was much decreased and the 500–600-nm bands increased during the annealing in this experiment (spectrum c).

On annealing matrices doped with 1% CO, no telling changes occurred in the optical spectra, apart from the growth of the 500–600-nm band if those had been bleached before. However, the IR spectra showed pronounced changes around 2100 and 1720  $\text{cm}^{-1}$ , i.e., the ketene and carbonyl stretching regions. This time, the extent of the spectral changes depended little on whether >515-nm photolysis was done before annealing or not.

## Theoretical Results and Discussion

**1. Methyl  $\alpha$ -Diazo(2-naphthyl)acetate.** The ESR experiments described above indicate very clearly the presence of at least two rotamers of  $^3\text{NCC}$  which could possibly arise directly from the corresponding rotamers in the diazo precursor, MDA. To find out whether the incipient population of the two carbene rotamers could be related to the conformational equilibrium in MDA, this equilibrium was calculated by optimizing the structures of the four conformers around the naphthyl– $\text{CN}_2$  and the  $\text{CN}_2$ –CO bonds.<sup>84</sup> The resulting energy differences were converted to  $\Delta G_{298}$  on the basis of the corresponding structures and vibrations.<sup>85</sup> The results, summarized in Table 1, indicate that, with regard to the  $\text{CN}_2$ –CO bond, the planar *E*-conformations are strongly favored over the *Z*-conformations where the naphthyl ring is twisted by  $\sim 50^\circ$ .

(84) In each case, the calculation was performed for the *Z*-conformation about the CO–OCH<sub>3</sub> bond. Experiments (Blom, C. E.; Günthard, Hs. H. *J. Am. Chem. Soc.* **1981**, *84*, 267) and calculations (Wang, X.; Houk, K. N. *J. Am. Chem. Soc.* **1988**, *110*, 1870–1872. Wiberg, K. B.; Laidig, K. E. *J. Am. Chem. Soc.* **1988**, *110*, 1872–1874) likewise show that the *Z*-conformations of esters are more stable than the *E*-conformations by 5–10 kcal/mol, due to unfavorable dipolar interactions in the latter.

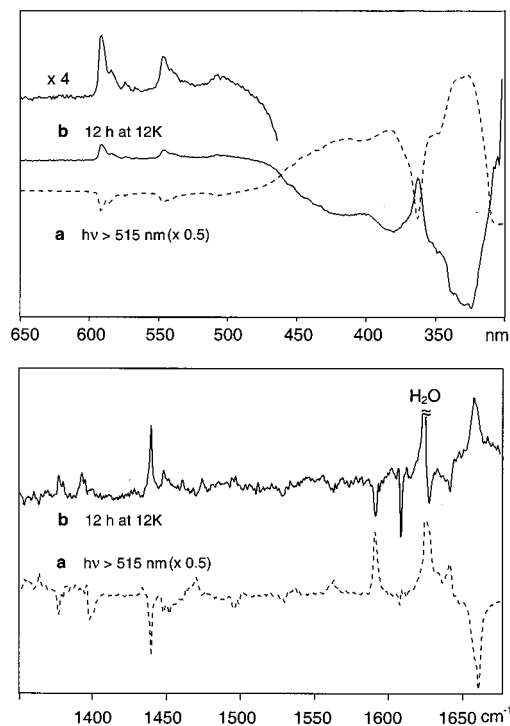
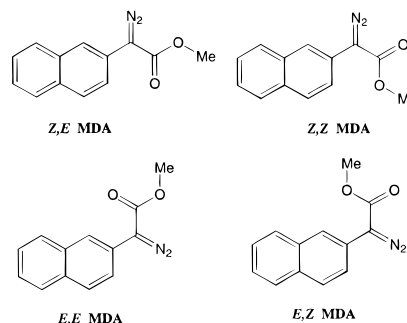


**Figure 5.** Changes in the optical spectra (top) and the IR spectra (bottom) upon allowing the sample giving spectrum c in Figure 1 to stand overnight in the dark at 12 K (a) and upon subsequent >515-nm bleaching (b).

**Table 1.** Relative Energies ( $\Delta E$ ), Room-Temperature Enthalpies ( $\Delta H_{298}$ ), Entropies ( $\Delta S_{298}$ ), and Free Energies ( $\Delta G_{298}$ ) of Different MDA Conformers from B3LYP/6-31G\* Calculations



| conformer          | $\Delta E$ ,<br>kcal/mol | $\Delta H_{298}$ ,<br>kcal/mol | $\Delta S_{298}$ , <sup>a</sup><br>cal/mol <sup>-1</sup> ·K | $\Delta G_{298}$ ,<br>kcal/mol | %<br>equil <sup>b</sup> |
|--------------------|--------------------------|--------------------------------|-------------------------------------------------------------|--------------------------------|-------------------------|
| ( <i>E,E</i> )-MDA | (0)                      | (0)                            | (0)                                                         | (0)                            | 62                      |
| ( <i>Z,E</i> )-MDA | 0.33                     | 0.32                           | +0.06                                                       | 0.30                           | 37                      |
| ( <i>E,Z</i> )-MDA | 2.37                     | 2.37                           | –0.50                                                       | 2.52                           | 0.5                     |
| ( <i>Z,Z</i> )-MDA | 2.37                     | 2.37                           | –0.50                                                       | 2.52                           | 0.5                     |

<sup>a</sup> Excluding contributions from (nearly) free internal rotations.<sup>85</sup>  
<sup>b</sup> Equilibrium composition.

Among the more stable  $\text{CN}_2$ –CO *E*-conformers, the one where the carbonyl group points toward the hydrogen in the 1-position of the naphthyl ring ((*E,E*)-MDA) is slightly favored over the one where it points to the hydrogen in the 3-position ((*Z,E*)-MDA). However, the energy difference between the two

(85) The calculation of the entropy contributions is problematic because of the very low barrier for rotation of the  $\text{CN}_2\text{COOMe}$  group relative to the naphthyl moiety, which gives rise to very low frequency twisting vibrations in all four conformers. In calculating  $\Delta G_{298}$  we assumed that this contribution (as well as that of the  $\text{CH}_3$  group's rotation) to the relative entropy cancels for the four conformers; i.e., we only took into account  $\Delta S_{\text{vib}}$  for the other vibrations. Note that, due to the small entropy and heat capacity differences between the different conformers,  $\Delta G$  will not exhibit a strong temperature dependence.

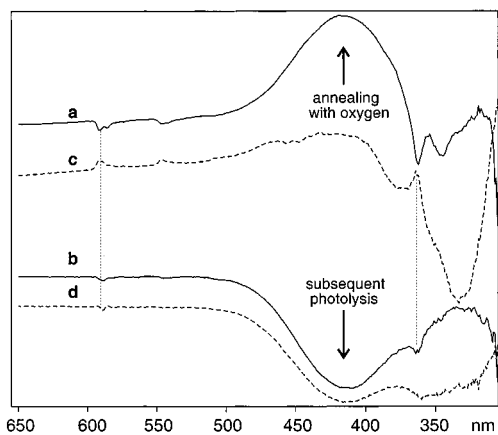


**Figure 6.** Changes in the optical spectra on annealing a sample doped with 0.2% O<sub>2</sub> (a) after photodeazotation of MDA or (c) after >515-nm bleaching of the resulting sample. Spectra b and d show the result of bleaching the broad 420-nm band of spectrum a or c, respectively.

is too small to be significant, so all one can say is that (*E,E*)- and (*Z,E*)-MDA should be present in similar amounts, whereas the other two conformations will only be present in minute quantities. If no conformational changes take place on deazotation, a similar ratio should be found in the incipient triplet carbenes, and the similar intensity within the pairs of ESR peaks indicates that this is effectively the case. As will be shown below, the presence of two rotamers manifests itself also in the IR spectrum of <sup>3</sup>NCC, albeit not as clearly as in the ESR spectra.

## 2. Triplet 2-Naphthyl(carbomethoxy)carbene (<sup>3</sup>NCC).

From the experiments described in the Experimental Results section and past experience from similar cases, we can easily assign the primary product of the photodeazotation of MDA to the triplet state of <sup>3</sup>NCC: it shows the ESR signals of a triplet, has the sharp visible bands typical of aromatic triplet carbenes,<sup>30,71</sup> is trapped very efficiently by O<sub>2</sub> to form a carbonyl oxide ( $\lambda_{\text{max}} = 420$  nm) which can readily be photodecomposed,<sup>30,86</sup> and reacts somewhat less efficiently with CO to give a ketoketene which is identified by its 1720- and 2100-cm<sup>-1</sup> bands.<sup>26,30,87,88</sup>

INDO/S-CI calculations on <sup>3</sup>NCC reproduce the observed bands at 590 (weak) and 360 nm (strong) reasonably well (Table 2, Figure 7) and predict additional weak transitions which may be responsible for the weak features observed at 430 and 410 nm (Figure 1, spectrum b). (These weak features are obscured in the difference spectrum due to the strong increase of the photoproduct absorptions in this region.) Also, the IR spectrum calculated for <sup>3</sup>NCC is in good agreement with the observed one. We will return to the issue of the IR spectrum after the conformational question discussed below is settled. At this point, it suffices to note that the “leading” IR band of <sup>3</sup>NCC is that at 1660 cm<sup>-1</sup> (see Figures 2, 4, and 5), which vanishes and reappears entirely in concert with the sharp bands in the visible.

The aforementioned ESR spectra reveal the presence of two major conformational isomers of <sup>3</sup>NCC (Figure 3). On the basis of the differential behavior of these isomers under thermal and photochemical conditions, the ESR transitions can be assigned for each conformer<sup>89</sup> and the zero-field splitting parameters can

(86) Sander, W.; Kirschfeld, A.; Kappert, W.; Muthusamy, S.; Kiselewsky, M. *J. Am. Chem. Soc.* **1996**, *118*, 6508.

(87) Toung, R. L.; Wentrup, C. *Tetrahedron* **1992**, *48*, 7641.

(88) Clemens, R. J.; Witzeman, J. S. *J. Am. Chem. Soc.* **1989**, *111*, 2191.

(89) Conformer A ((*Z,Z*)-<sup>3</sup>NCC):  $|D/hc| = 0.437$  cm<sup>-1</sup>,  $|E/hc| = 0.0357$  cm<sup>-1</sup>; Z<sub>1</sub> 1208 G, X<sub>2</sub> 4487 G, Y<sub>2</sub> 5915 G, and Z<sub>2</sub> 8074 G. Conformer B ((*E,Z*)-<sup>3</sup>NCC):  $|D/hc| = 0.415$  cm<sup>-1</sup>,  $|E/hc| = 0.0397$  cm<sup>-1</sup>; Z<sub>1</sub> 954 G, X<sub>2</sub> 4296 G, Y<sub>2</sub> 5867 G, and Z<sub>2</sub> 7839 G.; microwave frequency 9.510 GHz.

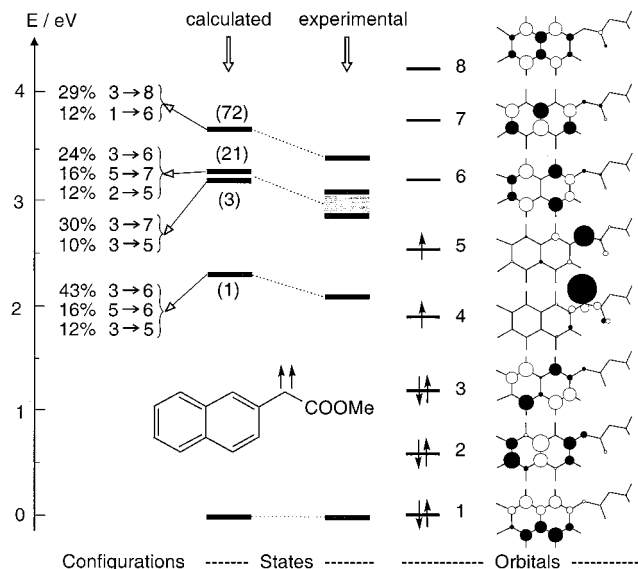


**Figure 7.** Graphical representation of the results of INDO/S-CI calculations on the excited states of <sup>3</sup>NCC. Black bars denote calculated energies and observed band maximums (cf. Table 2 and Figure 1). The leftmost column shows the composition of the excited states in terms of one-electron excitations involving the MOs depicted on the right. (Numbers in parentheses represent the calculated relative oscillator strengths.)

**Table 2.** Excited-State Energies ( $\Delta E$ ) and Oscillator Strengths ( $f$ ) of <sup>3</sup>NCC<sup>a</sup> by INDO/S-CI<sup>b</sup>

| excited state      | calcd $\Delta E$ , eV | $f$    | exptl $\Delta E$ , eV<br>( $\lambda_{\text{max}}$ , nm) |
|--------------------|-----------------------|--------|---------------------------------------------------------|
| 2 <sup>3</sup> A'' | 2.28                  | 0.0001 | 2.10 (590)                                              |
| 3 <sup>3</sup> A'' | 3.21                  | 0.0003 | 2.85 (435)                                              |
| 4 <sup>3</sup> A'' | 3.29                  | 0.0021 | 3.06 (405)                                              |
| 5 <sup>3</sup> A'' | 3.57                  | 0.0072 | 3.42 (362)                                              |
| 6 <sup>3</sup> A'' | 3.72                  | 0.0003 |                                                         |
| 7 <sup>3</sup> A'' | 3.78                  | 0.0564 |                                                         |

<sup>a</sup> At the B3LYP/6-31G\* geometry (see Figure 9). <sup>b</sup> Including singly and doubly excited configurations.

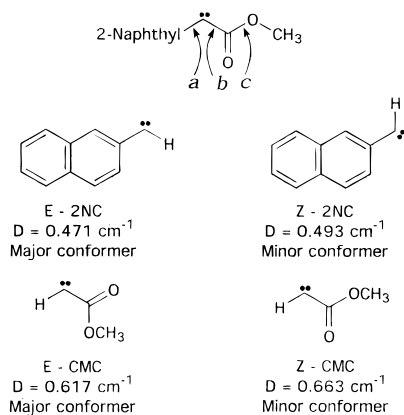
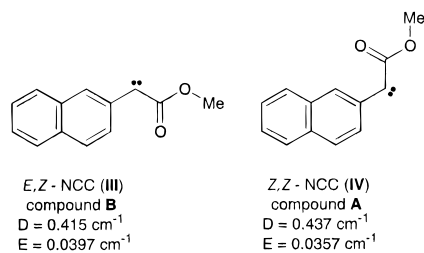
be computed using the best fit of the observed ESR transitions to the spin Hamiltonian.<sup>90</sup> In principle, <sup>3</sup>NCC might be expected to display eight low-energy conformations arising from restricted rotation about bonds a, b, and c in low-temperature matrixes (Chart 1).<sup>25</sup> In triplet carbenes with structural similarities to <sup>3</sup>NCC, conformational isomers associated with restricted rotation about bonds of types a and b, but not type c,<sup>84</sup> have been characterized by ESR spectroscopy. The model compounds 2NC,<sup>25,71,91,92</sup> (4-nitrophenyl)carbomethoxycarbene,<sup>28,31</sup> and carbomethoxycarbene (CMC)<sup>24,25</sup> provide a framework for discussing the triplet ESR spectra of <sup>3</sup>NCC. As expected, the *D* values of <sup>3</sup>NCC (0.437, 0.415 cm<sup>-1</sup>) are smaller than those of <sup>3</sup>2NC (0.493, 0.471 cm<sup>-1</sup>) because of the additional delocalization provided by the carbomethoxy substituent in <sup>3</sup>NCC. A similar relationship is observed between the *D* values of (4-nitrophenyl)-carbomethoxycarbene (0.453 cm<sup>-1</sup>)<sup>28,93</sup> and (4-nitrophenyl)-

(90) Wasserman, E.; Snyder, L. C.; Yager, W. A. *J. Chem. Phys.* **1964**, *41*, 1763.

(91) Trozzolo, A. M.; Wasserman, E.; Yager, W. A. *J. Am. Chem. Soc.* **1965**, *87*, 129.

(92) Senthilnathan, V. P.; Platz, M. S. *J. Am. Chem. Soc.* **1981**, *103*, 5503.

(93) The *D* value of the minor rotamer of triplet (4-nitrophenyl)-carbomethoxycarbene is not well determined. Only the X<sub>2</sub> and Y<sub>2</sub> transitions of the minor rotamer were detected. To estimate the *D* value for this species, the authors assumed that the Z<sub>1</sub> and Z<sub>2</sub> transitions were coincident with the corresponding transitions of the major rotamer

**Chart 1.** ESR Parameters of Different Carbene Conformers**Chart 2.** Assignment of the ESR Spectra in Figure 3 to Two Rotamers of  $^3\text{NCC}$ 

carbene ( $0.486 \text{ cm}^{-1}$ ).<sup>94</sup> The observed difference in  $D$  values between the two conformational isomers of  $^3\text{NCC}$  ( $\Delta D = 0.022 \text{ cm}^{-1}$ ) is similar to that observed for the isomers of  $^3\text{2NC}$  ( $\Delta D = 0.022 \text{ cm}^{-1}$ ), but smaller than that observed for isomers of  $^3\text{CMC}$  ( $\Delta D = 0.046 \text{ cm}^{-1}$ ).<sup>25</sup>

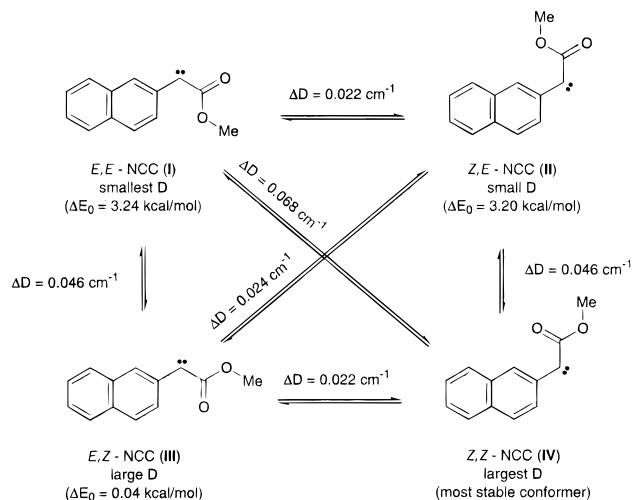
Assuming that the effects of the naphthyl and carbomethoxy substituents on the carbene  $D$  values can be assessed independently, one can predict the relative magnitudes of the  $D$  values for the four conformational isomers of  $^3\text{NCC}$  that arise from restricted rotation about bonds a and b (Scheme 1).<sup>95</sup> This analysis reveals three pairs of isomers that display  $\Delta D$  values that are consistent with experiment ( $\Delta D \sim 0.02 \text{ cm}^{-1}$ ): conformers **I** and **II**, conformers **II** and **III**, and conformers **III** and **IV**. (In Scheme 1, equilibrium arrows represent the elementary conformational processes that relate the various isomers. Horizontal or vertical arrows represent rotation about one C–C bond; diagonal arrows represent inversion at the carbene center.)

To distinguish between these three possible cases, we note that conformers **III** and **IV** correspond to the two lowest energy conformers computed for the starting diazo compound ((*E,E*)- and (*Z,E*)-MDA; see Table 1), as well as for the carbenes themselves ((*Z,Z*)- and (*E,Z*)- $^3\text{NCC}$ ).<sup>96</sup> Thus, we tentatively assign the higher field set of transitions to (*Z,Z*)- $^3\text{NCC}$  (**A**) and the lower-field set of transitions to (*E,Z*)- $^3\text{NCC}$  (**B**).<sup>97</sup> Inspection of the ESR spectra (Figure 3) reveals additional weak, in some cases overlapping, transitions that reproducibly appear in all

(94) Trozzolo, A. M.; Wasserman, E. in: ref 5, Vol. II, pp 185–206.

(95) Quantitative estimates for the zero-field splitting parameters of individual conformational isomers of triplet carbenes can often be obtained using a point spin model.<sup>25</sup> This simple model, unfortunately, is not suitable for quantitative assessment of carbalkoxycarbenes.<sup>25</sup> Since the point spin model is not appropriate to analyze the NCC isomers, the assumption of treating the effects of the substituents on the  $D$  values as additive represents an oversimplification.

(96) Note that, by virtue of the substituent priorities in the Cahn–Ingold–Prelog rules, there is a “reversal” in the *E/Z*-nomenclature in going from MDA to NCC. Thus, (*E,E*)-MDA yields (*Z,Z*)-NCC and (*E,Z*)-MDA gives (*Z,E*)-NCC (and vice versa).

**Scheme 1.** Differences in  $D$  Values and Relative Energies (B3LYP/6-31G\*, Including ZPE Differences) of the Four Conformers of  $^3\text{NCC}^a$ 

<sup>a</sup> For total energies and Cartesian coordinates, see Supporting Information.

spectra. One may reasonably attribute these signals to small amounts of the *E,E*- and *Z,E*-conformers of  $^3\text{NCC}$ . Definitive assignments, however, are not possible.

**3. Benzobicyclo[4.1.0]heptatrienes and Benzocycloheptatetraenes.** The assignment of the product that arises on bleaching of  $^3\text{NCC}$  and that almost completely reforms  $^3\text{NCC}$ , thermally at 12 K or by 450-nm irradiation, is less straightforward. In view of the closely analogous case of 2-naphthylcarbene<sup>71</sup> or other similar examples,<sup>72,98</sup> one is tempted to assign the second product to the carbomethoxy derivative of 2,3-benzobicyclo[4.1.0]hepta-2,4,6-triene (BHT-COOMe). However, as will be shown below, several reasons speak against bicyclo[4.1.0]heptatriene or cycloheptatetraene intermediates in the photolysis of  $^3\text{NCC}$ .

The observed *thermal* reversibility of the  $^3\text{NCC}$  photorearrangement at 12 K implies that this process occurs with a very low activation barrier and/or via quantum mechanical tunneling, in a manner directly analogous to the BHD  $\rightarrow$   $^3\text{OCD}$  rearrangement.<sup>72b</sup> The thermal ring-opening reaction of BHD  $\rightarrow$  OCD occurs via tunneling at  $T < 20 \text{ K}$  (experimental  $E_a = 2.6 \pm 0.2 \text{ kcal/mol}$ ,<sup>72b</sup> computed  $\Delta E^\ddagger = 6.7 \text{ kcal/mol}$ <sup>73</sup>). Recent high-level computational studies, however, reveal a significantly higher barrier of 15 kcal/mol for the closely related reversal of parent bicyclo[4.1.0]hepta-2,4,6-triene to singlet phenyl carbene.<sup>76,77</sup> There is no apparent reason this barrier should be much decreased by 2,3-benzannelation. (Benzannelation also protects BHT from ring opening to a cycloheptatetraene derivative, which prevails in the parent system,<sup>76</sup> because this process leads to a loss of resonance energy due to the formation of an *o*-quinoid structure.<sup>78</sup>) Unfortunately, the barrier for BHT  $\rightarrow$  2NC was not addressed in an otherwise comprehensive study of various naphthylcarbene isomers,<sup>78</sup> so we calculated the (singlet) potential energy surfaces for the 2NC–BHT rearrangement, both for the parent and the COOMe derivative (Figure 8).<sup>99</sup> The results show that cyclization, which is exothermic by 6.6 kcal/mol in 2-naphthylcarbene, becomes nearly thermoneu-

(97) The relative population of carbene conformers depends on the matrix material and temperature. This dependence is thought to arise by the influence of these factors on the conformational populations of the ground-state diazo precursor.<sup>92</sup>

(98) See, e.g.: Albers, R.; Sander, W.; Ottoson, C.-H.; Cremer, D. *Chem. Eur. J.* **1996**, *2*, 967.

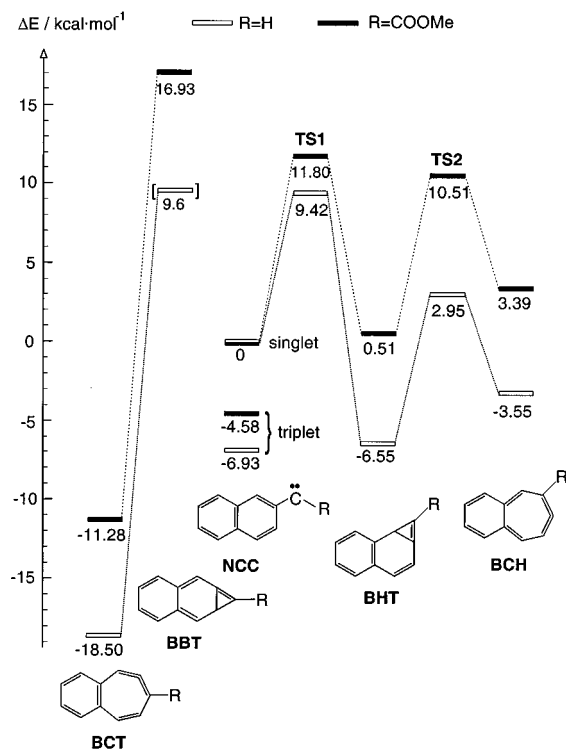


**Figure 8.** Schematic B3LYP/6-31G\* potential energy surfaces for the rearrangement of 2-naphthylcarbene and its carbomethoxy derivative, NCC, by cyclization to the tricyclic cyclopropenes, BHT and BBT, and the subsequent ring opening to the bicyclic allenes, BCH and BCT. All energies are relative to the singlet states of the carbenes and include zero-point energy corrections (total energies and Cartesian coordinates of all structures are available in Supporting Information).

tral in the COOMe derivative. Concomitantly, the calculated thermal barrier for the reverse reaction decreases from 16 kcal/mol for BHT  $\rightarrow$   $^1$ 2NC to 11.3 kcal/mol for BHT-COOMe  $\rightarrow$   $^1$ NCC.

Although the above predictions could be in error by (at most) a few kilocalories per mole, we note that the calculated barrier for the BHT-COOMe  $\rightarrow$  NCC rearrangement is  $\sim$ 6 kcal/mol higher than that calculated for the analogous BHD  $\rightarrow$  OCD rearrangement.<sup>100</sup> Both rearrangements take place with similar half-lives in Ar,<sup>101</sup> an observation that is inconsistent with the B3LYP prediction for the relative rates of the *thermally activated* rearrangements. However, the possibility that the BHT-COOMe  $\rightarrow$  NCC rearrangement occurs by quantum mechanical tunneling cannot be excluded, although this would seem to be rather unlikely in view of the large motion that the atoms of the COOMe group have to undergo in this process. (In a tunneling process, the reaction rate is more sensitive to barrier width than to barrier height.) Nevertheless, the thermal reactivity of the intermediate does not unequivocally rule out

(99) Our calculations revealed a discrepancy in the earlier computational study by Xie et al.<sup>78</sup> Our value of  $\Delta E(\text{BCH} - \text{BHT}) = 3.0$  kcal/mol disagrees with the value of 1.4 kcal/mol which can be gathered from Table 2 of ref 78 (both by B3LYP/6-31G\* after ZPE correction). The reason is that for BCH (**16** in the previous study) the ZPE difference of 0.8 kcal/mol was subtracted instead of added to the energy difference to triplet 2-naphthylcarbene. The B3LYP/6-31G\* entry for **16** should be 3.4 kcal/mol instead of 1.8 kcal/mol.

(100) To validate the B3LYP/6-31G\* procedure for this type of application, we calculated the barrier for the BHD–OCD rearrangement.<sup>37</sup> After ZPE correction, this turned out to be 5 kcal/mol at 0 K, 1.7 kcal/mol lower than a recent CASSCF/CASPT2 calculation.<sup>73</sup> If compared to the experimental  $E_a$  of 2.6 kcal/mol for the BHD–OCD rearrangement,<sup>72b</sup> even B3LYP appears to overestimate the barriers for such reactions.

(101) Sander et al. reported a half-life of  $165 \pm 30$  h at 9 K;<sup>72b</sup> we found  $\sim$ 48 h at 12 K.

**Table 3.** Excited-State Energies ( $\Delta E$ ) and Oscillator Strengths ( $f$ ) of BHT, BHT-COOMe, and BBT-COOMe<sup>a</sup> by INDO/S-CI<sup>b</sup>

| excited state | BHT             |      | BHT-COOMe       |      | BBT-COOMe       |      |
|---------------|-----------------|------|-----------------|------|-----------------|------|
|               | $\Delta E$ , eV | $f$  | $\Delta E$ , eV | $f$  | $\Delta E$ , eV | $f$  |
| 2 $^1$ A      | 4.60            | 0.01 | 4.47            | 0.04 | 3.16            | 0.03 |
| 3 $^1$ A      | 4.68            | 0.12 | 4.52            | 0.19 | 3.52            | 0.17 |
| 4 $^1$ A      | 4.99            | 0.10 | 4.86            | 0.14 | 4.36            | 0.14 |
| 5 $^1$ A      | 5.55            | 0.05 | 5.35            | 0.03 | 4.65            | 0.03 |

<sup>a</sup> At the B3LYP/6-31G\* geometries. <sup>b</sup> Including singly and doubly excited configurations.

BHT-COOMe as the photoproduct of  $^3$ NCC. In contrast, the spectroscopic evidence provided below for excluding BHT-COOMe (and other possible photoproducts) is compelling.

First, the reversible interconversion with  $^3$ NCC involves no detectable change in the IR spectrum between 1670 (C=O stretching frequency of  $^3$ NCC) and 2120  $\text{cm}^{-1}$  (C=C=O stretching frequency of 2-naphthylmethoxyketene). The distinctive C=C stretching vibration of parent BHT occurs around 1750  $\text{cm}^{-1}$ ,<sup>71</sup> and according to B3LYP/6-31G\* frequency calculations on BHT and its COOMe derivative,<sup>37</sup> carbomethoxy substitution shifts this band by  $\sim$ 40  $\text{cm}^{-1}$  to *higher* energy, (i.e., it would be expected at  $\sim$ 1800  $\text{cm}^{-1}$  in BHT-COOMe). However, the first noticeable change in the IR spectrum occurs at 1660  $\text{cm}^{-1}$ , i.e., some 90  $\text{cm}^{-1}$  *below* the occurrence of the C=C stretching vibration in BHT. This would imply a complete failure of the B3LYP/6-31G\* model for calculating vibrational spectra, which would be very surprising in view of the many successes that have recently been reported.<sup>76,102</sup>

Second, BHT shows no optical absorptions at longer wavelengths than 350 nm,<sup>71</sup> in accord with expectations for its phenylbutadiene chromophore. To place an estimate on the influence of the COOMe group, we carried out INDO/S-CI excited-state calculations (Table 3) which actually predict *hypsochromic* shifts of the first two electronic transitions on carbomethoxy substitution. (Note that INDO/S-CI predicts the position of the first UV band of BHT at 270 nm<sup>71</sup> (4.6 eV) quite accurately.)

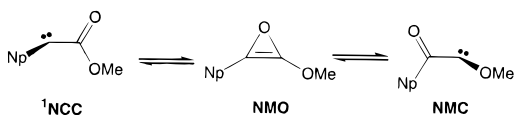
Third, we can exclude formation of the other possible vinylcarbene–cyclopropene rearrangement product, i.e., the COOMe derivative of 3,4-benzobicyclo[4.1.0]hepta-2,4,6-triene (BBT-COOMe). This species would be expected to show the strong 350–400-nm (3.1–3.5 eV) absorptions that are typical for *o*-quinoid chromophores,<sup>103</sup> in accord with INDO/S-CI calculations (see last columns of Table 3). Parent BBT has been ruled out on the same grounds in the recent study of the photorearrangement of 2-naphthylcarbene.<sup>71</sup> Apart from that, BBT-COOMe is calculated to lie  $\sim$ 17 kcal/mol higher in energy than BHT-COOMe; hence its formation cannot compete with that of the latter isomer due to loss of aromaticity. The absence of absorptions that are typical for *o*-quinoid chromophores also provides evidence to exclude the *o*-quinoid cycloheptatriene derivative BCH-COOMe (Figure 8) as the photoproduct of  $^3$ NCC. Finally, BCT-COOMe is excluded as the photoproduct of  $^3$ NCC because the rearrangement of BCT-COOMe  $\rightarrow$  NCC is calculated to be substantially endothermic (Figure 8).

(102) Rauhut, G.; Pulay, P. *J. Phys. Chem.* **1995**, *99*, 3093.

(103) McMahon, R. J.; Chapman, O. L. *J. Am. Chem. Soc.* **1987**, *109*, 683.

In sum, the combined evidence from IR and UV spectroscopy and the different quantum chemical calculations presented in this section force us to conclude that BHT-COOMe, BBT-COOMe, BCH-COOMe, and BCT-COOMe are not viable candidates for the photoproduct of  $^3\text{NCC}$ . Therefore, we have to turn to other hypotheses.

**4. 1-(2-Naphthyl)-2-methoxyoxirene (NMO) and 2-Naphthyl(methoxy)carbene (NMC).** Whenever carbonylcarbenes are involved in chemical reactions, consideration of the corresponding oxirenes and the isomeric carbonylcarbenes as possible reactive intermediates imposes itself. In the present case, the relevant species are NMO and NMC. As mentioned in the Introduction, electron-releasing substituents are expected to stabilize the electron-deficient singlet carbene relative to the electron-rich oxirene and thus lead to the disappearance of the



tiny barrier separating the two species in parent formylcarbene.<sup>64</sup> Indeed, all attempts to locate a minimum corresponding to NMO converged either to  $^1\text{NCC}$  or to  $^1\text{NMC}$  (except at the rather unreliable HF/3-21G level where NMO resides in a very shallow minimum). In contrast, a transition-state search revealed a saddle point corresponding to NMO whose imaginary normal mode was found to correspond to the expected reaction vector for the  $^1\text{NCC} \rightarrow ^1\text{NMC}$  interconversion.<sup>104</sup>

At the B3LYP/6-31G\* level, the  $^1\text{NCC} \rightarrow ^1\text{NMC}$  rearrangement is nearly thermoneutral ( $\Delta E_0 = +0.8$  kcal/mol). If we assume that the substituent on the other side of the C=O group does not influence the thermochemistry, this implies that the naphthyl and the methoxy substituents stabilize the singlet carbonylcarbene relative to the oxirene by similar amounts. In contrast, the oxirene appears to be doubly penalized by the two electron-releasing substituents, in that the energy difference between NMO and  $^1\text{NCC}$  is calculated to be 31.3 kcal/mol (30.0 kcal/mol including the ZPE difference).<sup>106</sup>

The above findings would seem to rule out both the oxirene (NMO) and the rearranged carbene ( $^1\text{NMC}$ ) as viable candidates for the photoproduct of  $^3\text{NCC}$ : NMO is not a stable intermediate, and the calculated barrier for the  $^1\text{NMC} \rightarrow ^1\text{NCC}$  reversal is too high to account for the observed thermal reversal of the photoproduct to  $^3\text{NCC}$ . In addition, INDO/S-CI calculations predict the first two transitions in the electronic absorption spectrum of  $^1\text{NMC}$  to be very weak and to occur in the UV (Table 4), in very poor agreement with the observed spectrum of the transient species formed upon  $>515$ -nm photolysis of

(104) Proof that this is indeed the transition state for the  $^1\text{NCC}$  to NMC interconversion could be obtained by an intrinsic reaction coordinate (IRC) calculation.<sup>105</sup> As this was too expensive to perform for the naphthyl system, we resorted to the corresponding phenyl derivative, which shows a saddle point of very similar structure associated with a similar activation energy relative to the (carbomethoxy)carbene (30.2 kcal/mol). An IRC calculation starting from 1-phenyl-2-methoxyoxirene did indeed show a smooth descent to phenyl(carbomethoxy)carbene in one direction and to benzoyl(methoxy)carbene in the other direction. We can see no reason this should be different in the naphthyl system.

(105) Gonzalez, C.; Schlegel, H. B. *J. Chem. Phys.* **1989**, *90*, 2154.

(106) We have carried out model calculations to probe the effect of a single electron-releasing substituent on the energetics of the singlet carbonylcarbene rearrangement. At the B3LYP/6-31G\* level, the barrier for the H-C-COOMe  $\rightarrow$  HCO-C-OMe reaction (which is exothermic by 9.2 kcal/mol) via methoxyoxirene is 24.3 kcal/mol, in accord with expectations. In contrast, the H-C-COPh  $\rightarrow$  HCO-C-Ph rearrangement ( $\Delta E_0 = -6.0$  kcal/mol) takes on a two-step course via a shallow oxirene minimum of much lower relative energy. A more in-depth study of this phenomenon is in progress (Matzinger, S.; Bally, T., to be published).

**Table 4.** Excited-State Energies ( $\Delta E$ ) and Oscillator Strengths ( $f$ ) of  $^1\text{NMC}$ <sup>a</sup> by INDO/S-CI<sup>b</sup>

| excited state  | $\Delta E$ , eV | $\lambda_{\text{max}}$ , nm | $f$    |
|----------------|-----------------|-----------------------------|--------|
| 2 $^1\text{A}$ | 3.72            | 333                         | 0.0016 |
| 3 $^1\text{A}$ | 3.99            | 311                         | 0.0091 |
| 4 $^1\text{A}$ | 4.44            | 274                         | 0.1471 |
| 5 $^3\text{A}$ | 5.49            | 226                         | 1.9078 |

<sup>a</sup> At the B3LYP/6-31G\* geometry of (*E*)- $^1\text{NMC}$  (see Figure 9).

<sup>b</sup> Including singly and doubly excited configurations.

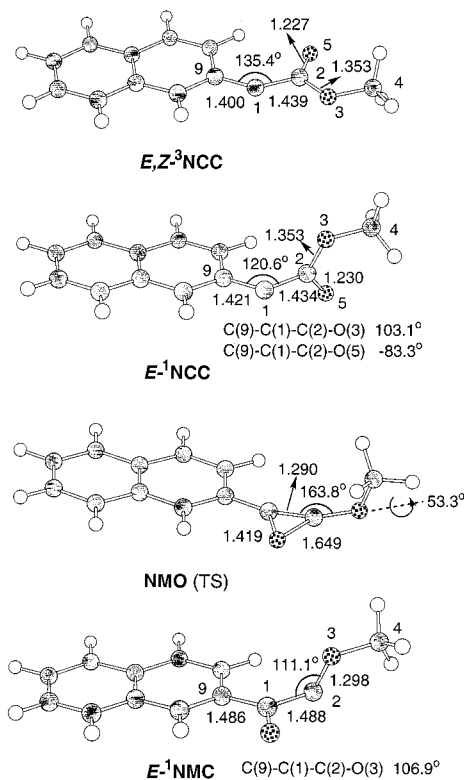


**Figure 9.** Geometries of (*E,Z*)- $^3\text{NCC}$ ,  $^1\text{NCC}$ , NMO, and  $^1\text{NMC}$  by B3LYP/6-31G\* (for total energies and Cartesian coordinates of all carbene conformers, see Supporting Information).

$^3\text{NCC}$  (cf. Figure 4, strong absorption at  $\sim 400$  nm). Finally, it will be shown below that the observed IR spectrum also speaks against an assignment to  $^1\text{NMC}$ .

**5. Singlet 2-Naphthyl(carbomethoxy)carbene ( $^1\text{NCC}$ ).** In view of the conclusions in the preceding two sections, the remaining logical candidate for the photoproduct of  $^3\text{NCC}$  is the singlet state of the same carbene,  $^1\text{NCC}$ . This species differs in an important way from  $^3\text{NCC}$  in that the carbomethoxy group assumes a *perpendicular* conformation to the naphthylcarbene plane (Figure 9) to avoid destabilization of the empty carbenic 2p atomic orbital by the electron-withdrawing carbonyl group. This feature of carbonylcarbenes was realized more than 20 years ago<sup>32–34,107</sup> and was later confirmed, computationally, to prevail in carbohydroxycarbenes.<sup>35,36</sup>

To find out whether this geometry change could create a barrier for the relaxation of the singlet to the triplet ground state of NCC, we calculated the potential energy surfaces for both states as a function of the dihedral angle between the COOMe and the naphthylcarbene planes and as a function of the bond angle at the carbenic carbon. The results of this computational study are depicted in Figure 10, which shows that, at the singlet geometry,  $^3\text{NCC}$  is an excited state and that the lowest point of

(107) Strausz, O. P.; Gosavi, R. K.; Denes, A. S.; Czismadia, I. G. *J. Am. Chem. Soc.* **1976**, *98*, 4784.

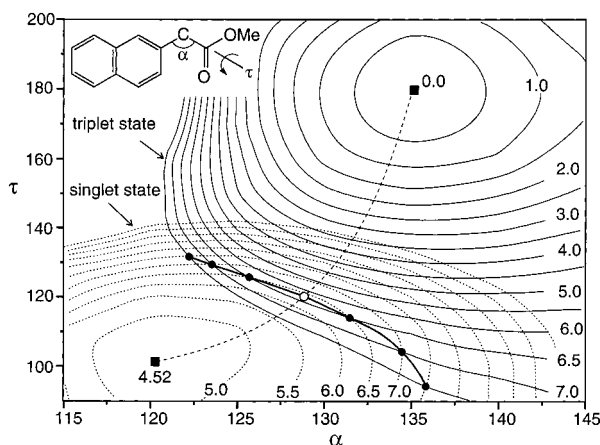


**Figure 10.** Potential energy surfaces for  $^1\text{NCC}$  (dashed) and  $^3\text{NCC}$  (solid lines) as a function of the angle  $\alpha$  at the carbenic carbon and the dihedral angle  $\tau$  between the COOMe group and the naphthylcarbene plane (equidistance of contour lines is 0.5 kcal/mol). The filled circles denote points of intersection of the two surfaces; the open circle is the lowest point on the line of intersection,  $\sim 2$  kcal/mol above  $^1\text{NCC}$ . The dashed line joining the minimums (squares) represents the minimum energy pathway. The surfaces were calculated on the basis of a grid of points in  $5^\circ$  increments of  $\alpha$  and  $10^\circ$  increments of  $\tau$  (geometries not optimized).

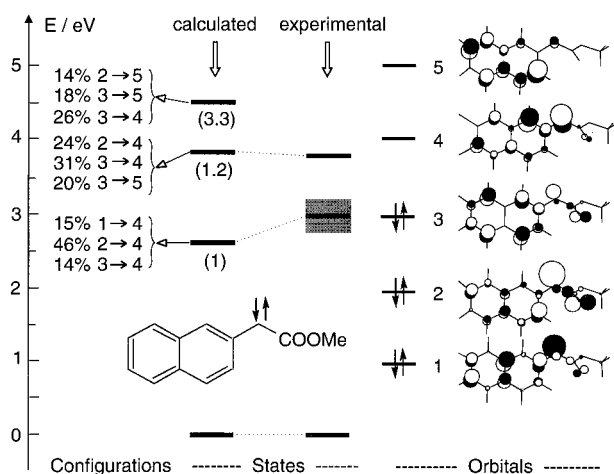


**Figure 11.** Graphical representation of the results of INDO/S-CI calculations on the excited states of  $^1\text{NCC}$ . Black bars denote calculated energies and observed band maximums (cf. Table 5 and Figure 1). The leftmost column shows the composition of the excited states in terms of one-electron excitations involving the MOs depicted on the right. (Numbers in parentheses represent the calculated relative oscillator strengths).

intersection between the two surfaces lies indeed 2 kcal/mol above the  $^1\text{NCC}$  minimum. As it was impossible to carry out full geometry optimizations at every  $\alpha/\tau$  grid point which was used in the construction of the surfaces in Figure 10, this number should be taken with a grain of salt. Apart from that, it is unclear how this value relates to the thermochemical activation parameters for the  $^1\text{NCC} \rightarrow ^3\text{NCC}$  relaxation process, but it is nevertheless compatible with a postulated assignment of the  $^3\text{NCC}$  photoproduct to  $^1\text{NCC}$ , an assignment that we shall try to substantiate below.

One of the distinct features of the photoproduct of  $^3\text{NCC}$  is its broad absorption around 420 nm. As INDO/S-CI provided a rather reasonable description of the electronic structure of  $^3\text{NCC}$ , we applied the same method to  $^1\text{NCC}$ . Indeed, INDO/S-CI predicts a rather strong transition in this region, albeit  $\sim 0.3$  eV too low, plus another one of similar intensity at 3.8 eV (325

**Table 5.** Excited-State Energies ( $\Delta E$ ) and Oscillator Strengths ( $f$ ) of  $^1\text{NCC}^a$  by INDO/S-CI<sup>b</sup>

| excited state  | calcd $\Delta E$ , eV | $f$    | exptl $\Delta E$ , eV ( $\lambda_{\text{max}}$ , nm) |
|----------------|-----------------------|--------|------------------------------------------------------|
| 2 $^1\text{A}$ | 2.66                  | 0.0382 | $\sim 3.0$ (410)                                     |
| 3 $^1\text{A}$ | 3.80                  | 0.0442 | $\sim 3.8$ (325)                                     |
| 4 $^1\text{A}$ | 4.44                  | 0.1262 |                                                      |
| 5 $^3\text{A}$ | 4.58                  | 0.1670 |                                                      |

<sup>a</sup> At the B3LYP/6-31G\* geometry of (*E*)- $^1\text{NCC}$  (see Figure 9).

<sup>b</sup> Including singly and doubly excited configurations.

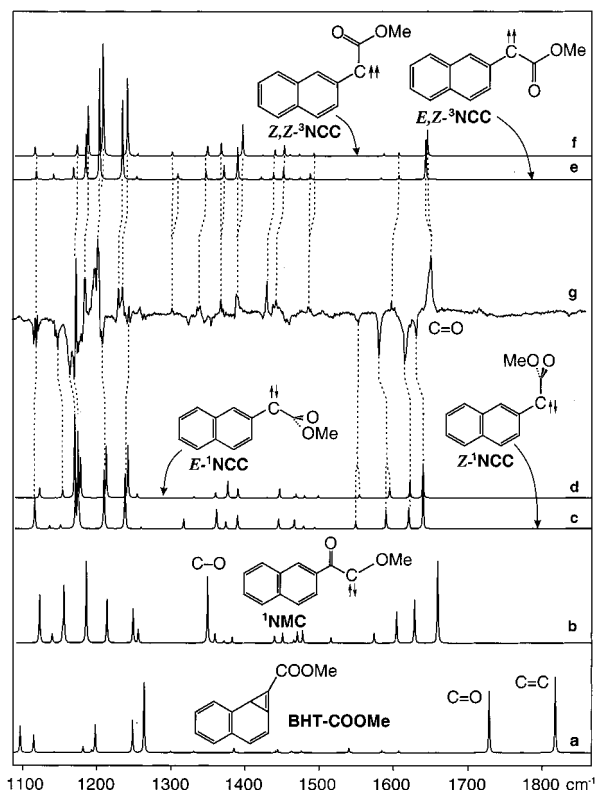


**Figure 12.** IR spectra computed for BHT-COOMe (a),  $^1\text{NMC}$  (b),  $^1\text{NCC}$  (c, d), and  $^3\text{NCC}$  (e, f), juxtaposed with the (inverted) experimental difference spectrum (c - b) of Figure 2 (g). B3LYP/6-31G\* frequencies scaled by 0.97.

nm) where the experimental spectrum indeed shows also a band (Table 5, Figure 11). Thus, INDO/S-CI supports the assignment of  $^1\text{NCC}$  as the photoproduct of  $^3\text{NCC}$ .

IR spectra also support the assignment of  $^1\text{NCC}$  as the photoproduct of  $^3\text{NCC}$ . Figure 12 depicts the difference spectrum (1100–1900  $\text{cm}^{-1}$ ) for the re-formation of  $^3\text{NCC}$  from the photoproduct. This experimental spectrum is compared with spectra computed (B3LYP/6-31G\*) for (*Z,Z*)- and (*E,Z*)- $^3\text{NCC}$  (the two conformers that had been identified from the ESR spectra), (*E*)- and (*Z*)- $^1\text{NCC}$ , and spectra computed for alternative photoproducts of  $^3\text{NCC}$  ( $^1\text{NMC}$ , BHT-COOMe). Clearly, the main features of the IR spectrum of the photoproduct (peaks pointing downward in spectrum g of Figure 12) agree reasonably well with the predictions for  $^1\text{NCC}$  (Figure 12, spectra c and d). Although some of the smaller features between 1300 and 1500  $\text{cm}^{-1}$  are lost because they coincide in part with stronger peaks of  $^3\text{NCC}$ , the important triad of peaks at 1591, 1626, and 1641  $\text{cm}^{-1}$  and the group of bands around 1200  $\text{cm}^{-1}$  are well reproduced by B3LYP.

In contrast, the experimental spectrum is entirely incompatible with the predictions for the tricyclic cyclopropane, BHT-COOMe (spectrum a; note in particular the absence of any peaks

between 1700 and 1850  $\text{cm}^{-1}$ ). In the case of  $^1\text{NMC}$  (spectrum b), the differences are more subtle, but the complete absence of the rather intense C–O stretch predicted at  $\sim 1350 \text{ cm}^{-1}$  indicates, in addition to the evidence provided in the previous section, that the experimental spectrum is incompatible with  $^1\text{NMC}$ .

We take this occasion to return briefly to  $^3\text{NCC}$ , whose IR spectrum is also very satisfactorily reproduced by B3LYP (Figure 12, spectra e and f) perhaps with the exception of the relative intensities of some of the smaller peaks that do not agree optimally with those in the experimental spectrum. A closer inspection reveals that many of the peaks are split into pairs in accord with the predictions for the two conformers of  $^3\text{NCC}$  (see in particular the region around  $1200 \text{ cm}^{-1}$ ) so that the presence of these two species which had become evident from the ESR spectra can also be detected by IR.

We do not claim that the above spectroscopic evidence represents a structural proof, but at least it is in good accord with our proposed assignment of  $^1\text{NCC}$  to the metastable photoproduct of  $^3\text{NCC}$ . On the basis of the available experimental results, and their concord with the theoretical findings, we propose that this is indeed the first example of a reversible interconversion between a triplet ground-state carbene with its metastable singlet counterpart. This behavior is made possible by virtue of the carbomethoxy group's preference for a perpendicular conformation in the singlet state.

A very similar phenomenon was recently reported by Berson and co-workers, who found that the singlet and triplet states of dimethylenepyrrole diradicals can be stabilized separately.<sup>108,109</sup> Berson conjectured that the energetic ordering of spin states depends critically on the conformation of the tosyl substituent at the pyrrole nitrogen atom. Hence, intersystem crossing is coupled to the conformational isomerization of this substituent, a process that may be quite slow in solid matrixes. In contrast to the case of the dimethylenepyrrole diradicals, where both spin states were found to be thermally stable up to 90 K, the S/T gap in NCC makes for a sufficient thermochemical driving force to permit observation of slow S  $\rightarrow$  T conversion even at 12 K.<sup>110</sup>

Finally, we briefly address the question of why the decay of the diazo precursor, MDA, which occurs presumably from the singlet excited state, leads almost exclusively to the triplet carbene (cf. Figure 1). The reason for this may be that the predominant conformers of ground-state MDA are entirely planar. If excitation does not result in any conformational change,<sup>111</sup> the incipient carbene will also arise in a planar conformation where the singlet is much less stable than the triplet (on enforcing planarity in  $^3\text{NCC}$ , the S/T splitting is  $\sim 17 \text{ kcal/mol}$  by B3LYP/6-31G\*). If intersystem crossing is more rapid than decay along a singlet pathway to a  $90^\circ$  twisted geometry (which may furthermore be impeded considerably in an argon matrix), then the first stable product of the MDA photolysis will be the triplet carbene, as observed.

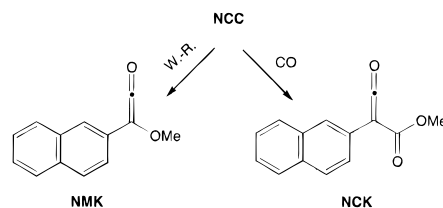
**6. Other Photoproducts.** Along with the formation of  $^3\text{NCC}$ , photolysis of the diazo precursor, MDA, produces two distinct IR peaks, a double-humped one at  $1846 \text{ cm}^{-1}$  and another closely spaced group at  $2120 \text{ cm}^{-1}$  (Figure 2, spectrum b – a).

(108) Bush, L. C.; Heath, R. B.; Feng, X. W.; Wang, P. A.; Maksimovic, L.; Song, A. I.; Chung, W.-S.; Berinstain, A. B.; Scaiano, J. C.; Berson, J. A. *J. Am. Chem. Soc.* **1997**, *119*, 1406.

(109) Bush, L. C.; Maksimovic, L.; Feng, X. W.; Lu, H. S. M.; Berson, J. A. *J. Am. Chem. Soc.* **1997**, *119*, 1416.

(110) Berson's diradicals were designed to have nearly degenerate singlet and triplet states.<sup>108,109</sup> Consequently, they lack a thermochemical driving force for S  $\rightarrow$  T or T  $\rightarrow$  S conversion which could be part of the reason it is not observed.

Neither peak changes appreciably on  $>515\text{-nm}$  photolysis of  $^3\text{NCC}$ , but both peaks increase slightly in intensity on  $450\text{-nm}$  photolysis of  $^1\text{NCC}$ . The peak at  $2120 \text{ cm}^{-1}$  can readily be assigned to 2-naphthyl(methoxy)ketene (NMK) resulting from Wolff rearrangement. NMK may be formed initially from the minor conformers of MDA (Z,Z and E,E), perhaps via a concerted Wolff rearrangement, and as one of several minor photochemical products in subsequent bleachings of the (perpendicular)  $^1\text{NCC}$ . NMK is distinct from 2-naphthyl(carbo-

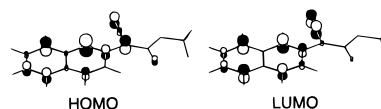


methoxy)ketene (NCK), which is formed in the course of the CO trapping studies. (The ketene stretching vibration of NCK appears to coincide with, and thus be largely masked by, the strong  $2100\text{-cm}^{-1}$  band of the diazo precursor.) Neither ketene appears to manifest itself detectably in the optical spectrum above 300 nm.

The other peak at  $1846 \text{ cm}^{-1}$  is more enigmatic because several species could conceivably be responsible for it, notably the valence isomers BHT- and BBT-COOMe as well as the cyclic allenes that result from ring opening of the former (Figure 8). However, all of these compounds have, in addition to the cyclopropene (BHT/BBT) or the cyclic allene stretch (BCH/BCT), an associated carbonyl stretching frequency around  $1750 \text{ cm}^{-1}$  from the COOMe group which should rise in concert with the former. However, the difference spectra for photolysis of MDA show no such peaks and the calculated spectra for the above four compounds are generally incompatible with that of the species associated with the  $1846\text{-cm}^{-1}$  peak.

The probable identity of this product revealed itself on  $313\text{-nm}$  photolysis which led to the complete bleaching of the  $1846\text{-cm}^{-1}$  peak in the IR along with a few others at lower energies of which one at  $1105 \text{ cm}^{-1}$  was most prominent. More importantly, the bleaching of this species led to a strong increase of the IR absorption of  $\text{CO}_2$ , which indicates that the species under investigation must be able to lose this fragment. One compound that fulfills this role is 2-(2-naphthyl)propiolactone (NPL). The  $\beta$ -lactone structure would be expected to display a high-frequency carbonyl stretch, in good accord with the experimentally observed value of  $1846 \text{ cm}^{-1}$ .<sup>112</sup> NPL represents a logical photoproduct of  $^1\text{NCC}$ , arising as a result of formal insertion of the carbene center into a C–H bond of the methoxy group.<sup>113</sup> This  $\beta$ -lactone would be expected to suffer photo-

(111) Full geometry optimizations of MDA in its lowest excited singlet state (by CIS or CASSCF) turned out to be computationally too demanding. However, we note that the HOMO of MDA is  $\pi$ -antibonding along the naphthyl– $\text{CN}_2$  bond whereas the LUMO is slightly bonding. Hence, excitation should lead to an increase in the  $\pi$  bond order along

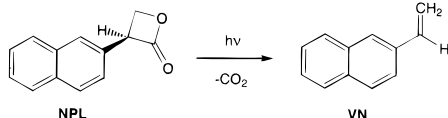


this bond which makes it very probable that the planar conformation of the naphthyl– $\text{CN}_2$  moiety is preserved in the first excited state.

(112) Socrates, G. *Infrared Characteristic Group Frequencies*; Wiley-Interscience: Chichester, 1980.

(113)  $\beta$ -Lactone formation has been observed previously on thermolysis of diazo esters: Richardson, D. C.; Hendrick, M. E.; Jones, M. *J. Am. Chem. Soc.* **1971**, *93*, 3790.

chemical loss of CO<sub>2</sub> to give 2-vinylnaphthalene (VN), which



unfortunately has no IR absorptions with an intensity commensurate with that of C=O stretches, and hence it is not surprising that it does not manifest itself clearly as a photofragment. However, in the flash photolysis studies described in the accompanying paper of Wang *et al.*,<sup>16</sup> VN was observed as a final product of the photolysis of MDA.

## Conclusions

On irradiation into its weak visible absorption band, <sup>3</sup>NCC is converted to a photoproduct with a broad absorption at 420 nm. Concurrently, the ESR signals of <sup>3</sup>NCC disappear, which indicates that the photoproduct is a singlet species. On photolysis at 450 nm or upon standing overnight at 12 K in the dark, <sup>3</sup>-NCC is re-formed almost quantitatively. We showed, by a combination of different spectroscopic and theoretical methods, that the above photoproduct is identical to the singlet state of the same carbene, <sup>1</sup>NCC, which is marginally protected from spontaneous decay to the triplet ground state by a pronounced conformational change of the COOMe group. The ester group is coplanar with the naphthylcarbene moiety in <sup>3</sup>NCC but

assumes a perpendicular conformation in <sup>1</sup>NCC to avoid destabilization of the formally vacant carbenic 2p atomic orbital by the electron-withdrawing carbonyl group. A very similar case of “conformational control of the spin state” has recently been found in dimethylenepyrrole diradicals.<sup>108</sup> However, to our best knowledge, the example of 2-naphthyl(carbomethoxy)carbene is the first case in which a metastable singlet state and its slow thermal conversion to the triplet ground state have been observed spectroscopically.

**Acknowledgment.** This work is part of Project 2028-047212.96 of the Swiss National Science Foundation and Grant CHE-9301025 of the U.S. National Science Foundation. We are very indebted to Prof. Matthew Platz (Ohio State University) for raising the problem of the enigmatic photoproduct of <sup>3</sup>NCC and for his continued interest in the resolution of the problem. We thank him as well as Prof. John Toscano (Johns Hopkins University) for the open exchange of data and manuscripts which made it possible to present our results jointly. Finally, we gratefully acknowledge the help of Dr. Stephan Matzinger (University of Fribourg) in locating the oxirene transition state for the NCC–NMC interconversion and for the IRC calculations on the phenyl derivative.

**Supporting Information Available:** Tables containing the B3LYP/6-31G\* optimized Cartesian coordinates, total energies, and thermal corrections of all stationary points (minimums and transition states) discussed in this study, in ASCII format. This material is available free of charge via the Internet at <http://pubs.acs.org>.

JA983277W